

# Probing the accretion disk structure by the twin kHz QPOs and spins of neutron stars in LMXBs

D. H. Wang<sup>1,2\*</sup>, C. M. Zhang<sup>3</sup>, Y. J. Lei<sup>3</sup>, L. Chen<sup>4</sup>, J. L. Qu<sup>5</sup>, Q. J. Zhi<sup>1,2</sup>

<sup>1</sup>*School of Physics and Electronic Science, Guizhou Normal University, Guiyang, 550001, China*

<sup>2</sup>*NAOC-GZNU Astronomy Research and Education Center, Guizhou Normal University, Guiyang, 550001, China*

<sup>3</sup>*National Astronomical Observatories, Chinese Academy of Sciences, Beijing, 100012, China*

<sup>4</sup>*Astronomy Department, Beijing Normal University, Beijing, 100875, China*

<sup>5</sup>*Institute of High Energy Physics, Chinese Academy of Sciences, Beijing, 100049, China*

Released 201608

## ABSTRACT

We analyze the relation between the emission radii of twin kilohertz quasi-periodic oscillations (kHz QPOs) and the co-rotation radii of the 12 neutron star low mass X-ray binaries (NS-LMXBs) which are simultaneously detected with the twin kHz QPOs and NS spins. We find that the average co-rotation radius of these sources is  $\langle r_{\text{co}} \rangle \sim 32$  km, and all the emission positions of twin kHz QPOs lie inside the co-rotation radii, indicating that the twin kHz QPOs are formed in the spin-up process. It is noticed that the upper frequency of twin kHz QPOs is higher than NS spin frequency by  $\geq 10\%$ , which may account for a critical velocity difference between the Keplerian motion of accretion matter and NS spin that is corresponding to the production of twin kHz QPOs. In addition, we also find that  $\sim 83\%$  of twin kHz QPOs cluster around the radius range of  $15 - 20$  km, which may be affected by the hard surface or the local strong magnetic field of NS. As a special case, SAX J1808.4-3658 shows the larger emission radii of twin kHz QPOs of  $r \sim 21 - 24$  km, which may be due to its low accretion rate or small measured NS mass ( $< 1.4 M_{\odot}$ ).

**Key words:** X-rays: binaries–binaries: close–stars: neutron–accretion: accretion disks

## 1 INTRODUCTION

Kilohertz quasi-periodic oscillations (kHz QPOs) are the particular phenomena in neutron star low mass X-ray binaries (NS-LMXBs) (van der Klis 2006; Liu et al. 2007; Walter et al. 2015) and were firstly discovered by Rossi X-ray Timing Explorer (RXTE) (van der Klis et al. 1996; Strohmayer et al. 1996). These high-frequency QPOs usually occur in pairs (i.e. upper  $\nu_2$  and lower  $\nu_1$ ) with the frequency range of  $\simeq 100 - 1200$  Hz (see van der Klis 2000, 2006, 2016 for a review), and have been detected in all subclasses of NS-LMXB, i.e. the less luminous Atoll and high luminous Z sources (see Hasinger & van der Klis 1989 for the Atoll and Z definitions). Such a fast X-ray variability is a powerful tool to explore the effects of general relativity in a strong gravity regime (Miller et al. 1998; Stella & Vietri 1999; Miller & Miller 2015), constrain the NS Mass-Radius relation (Miller et al. 1998; Miller 2002; Zhang 2004; Zhang & Wang 2013) and

probe the accreting flow and magnetosphere-disk structure in LMXBs (Kluźniak et al. 1990; Kluźniak & Abramowicz 2001; Abramowicz et al. 2003a,b; Alpar 2012; Peille et al. 2014).

The frequencies of the twin kHz QPOs show a non-linear relation (Belloni et al. 2005; Zhang et al. 2006a; Belloni et al. 2007), and the properties of them are also correlated with other timing and spectral features, such as the positions in the X-ray color-color diagram (e.g., Wijnands et al. 1997a,b; Homan et al. 2002), the photon indexes of the energy spectrum (Kaaret et al. 1998), the noise features (Ford & van der Klis 1998), the X-ray luminosity (Méndez et al. 1999; Ford et al. 2000). In addition, the quality factors and *rms* amplitudes of the kHz QPOs are found to be dependent of the QPO frequency as well (e.g., Méndez et al. 2001; Wang et al. 2012). Moreover, the lower kHz QPO frequency correlates with the low-frequency (i.e. HBO, see van der Klis 2006) and they follow a tight relation, which has been also found in the accreting white dwarf binaries (Psaltis et al. 1999; Belloni et al. 2002; Warner & Woudt 2002; Mauche 2002).

\* wangdh@gznu.edu.cn, zhangcm@bao.ac.cn

Various theoretical models suggest that kHz QPOs reflect the orbital motion of matter at some preferred radius close to NS in LMXBs (Miller et al. 1998; Stella & Vietri 1999; Osherovich & Titarchuk 1999; Lamb & Miller 2001; Zhang 2004), and their frequencies are identified with various characteristic frequencies in the inner accretion flows or their resonances (Kluźniak & Abramowicz 2001; Abramowicz et al. 2003a,b; Török et al. 2005; Stuchlík et al. 2015).

The relativistic precession model (Stella & Vietri 1999; Stella et al. 1999) and Alfvén wave oscillation model (Zhang 2004) emphasize the influence of the strong gravitational field regime and magnetic field near NS, respectively, which have made the consistent description of the model with the observed data (Wang et al. 2013).

The emission position of the kHz QPOs provides a probe into the physical environment near the NS in LMXBs. Wang et al. (2015) analyze the relation between the emission radius of the kHz QPOs and the NS radius based on the Alfvén wave oscillation model, and find that most kHz QPOs emit at the position several kilometers away from the NS surface. Besides these, the relation between the emission radius of kHz QPOs and co-rotation radius of NS is helpful to understand the relative velocity between the accretion flow and NS spin, which can further be used to investigate the accretion environment of NS-LMXBs that arises the kHz QPOs. There are  $\sim 30$  LMXBs to have shown NS spins (van der Klis 2016), some of which have been detected with the spin period derivative (Burderi et al. 2006; Burderi & Di Salvo 2013; Walter et al. 2015). There are a dozen of NS-LMXBs to show both the twin kHz QPOs and NS spins (see Table 1), from which the emission radii of kHz QPOs and co-rotation radii of the sources can be inferred. The goal of this paper is to investigate the emission environments of kHz QPOs while comparing with the co-rotation radius of NS, and infer the production mechanisms of twin kHz QPOs.

The structure of the paper is as follows: In § 2, we introduce the twin kHz QPOs and NS spin data adopted in analysis. In § 3 we infer the emission radii of kHz QPOs and analyze its relation with the co-rotation radius. In § 4 we present the discussions and conclusions.

## 2 THE SAMPLE OF PUBLISHED TWIN KHZ QPO FREQUENCIES AND NS SPIN FREQUENCIES

We searched the published literature for the sources with both the detected twin kHz QPO frequencies and NS spin frequencies, and found that 12 sources satisfy the above conditions. These samples have been detected with 201 pairs of twin kHz QPOs as shown in Table 1 with the references, where the 26 pairs are taken from the accreting millisecond X-ray pulsars, and the 175 ones from Atoll sources. The NS spin frequencies of the 12 sources are taken from either periodic or nearly periodic X-ray burst oscillations (van der Klis 2000, 2006).

## 3 EMISSION RADIUS OF TWIN KHZ QPOS AND CO-ROTATION RADIUS

### 3.1 Emission radius of twin kHz QPOs

In this paper the both lower and upper kHz QPOs in one pair kHz QPOs are assumed to occur at the same radius, and the upper kHz QPO frequency  $\nu_2$  is assumed as the Keplerian orbital frequency  $\nu_K$  (e.g. Stella & Vietri 1999; Zhang 2004; van der Klis 2006):

$$\nu_2 = \nu_K = \sqrt{\frac{GM}{4\pi^2 r^3}}, \quad (1)$$

where  $G$  is the gravitational constant,  $M$  is the NS mass and  $r$  is the Keplerian orbital radius, i.e. the emission radius of the kHz QPOs referring to the center of NS. By solving equation (1), the radius  $r$  can be derived as:

$$\begin{aligned} r &= \left(\frac{GM}{4\pi^2}\right)^{1/3} \nu_2^{-2/3} \\ &\approx 19(\text{km}) \left(\frac{M}{1.6 M_\odot}\right)^{1/3} \left(\frac{\nu_2}{900 \text{ Hz}}\right)^{-2/3}, \end{aligned} \quad (2)$$

where the mass  $1.6 M_\odot$  is the average value of the millisecond pulsars (Zhang et al. 2011), and frequency 900 Hz is the average frequency of the upper kHz QPOs (see Wang et al. 2014 for the details). It is thought that kHz QPOs reflect the motion of matter in orbit at the inner accretion disk radius (or the magnetosphere-disk radius  $r_m$ , see van der Klis 2006), i.e.  $r \sim r_m$ . The magnetosphere-disk radius  $r_m$  is defined as the radius where the magnetic energy of NS becomes comparable to the kinetic energy of the accretion gas:

$$r_m = \xi r_A, \quad (3)$$

where  $\xi$  is a constant factor of  $\sim 0.5$  in the thin accretion disk and  $r_A$  is the Alfvén radius (Ghosh & Lamb 1979; Shapiro & Teukolsky 1983) ( $\xi \sim 1$  and  $r_m \sim r_A$  in the spherical accretion, see Bhattacharya & van den Heuvel 1991). It is known that NS is in the spin-up state when  $r_m < r_{co}$  while NS is in the spin-down state when  $r_m > r_{co}$  (or  $r_A > r_{co}$  for  $\xi \sim 1$ , see Bhattacharya & van den Heuvel 1991 for the details).

We infer the emission radii of the kHz QPOs in Table 1 by equation (2) with the detected  $\nu_2$  values and the assumed NS mass of  $1.6 M_\odot$ , where the NS mass of SAX J1808.4-3658 is adopted as  $1.4 M_\odot$  by referring to its measured value (Elebert et al. 2009). The ranges of the inferred emission radii of kHz QPOs of the 12 sources and their corresponding cumulative distribution function (CDF) curves are shown in Table 1 and Fig.1, respectively. We also show the CDF curve of the emission radii of all kHz QPOs ( $r \sim 15 - 36$  km) in Fig.2 (a), from which it can be seen that most emission radii cluster around the radius range of  $\sim 15 - 20$  km ( $\sim 83\%$  of the data), the rest of which mainly results from the source SAX J1808.4-3658 and XTE J1807.4-294 with the larger emission radii of  $\sim 21 - 24$  km and  $\sim 25 - 36$  km, respectively.

### 3.2 Co-rotation radius

The co-rotation radius  $r_{co}$  of the NS-LMXB (Bhattacharya & van den Heuvel 1991) is the radial distance at where the Keplerian orbital frequency equals

**Table 1.** Emission radii of twin kHz QPOs and co-rotation radii of NS-LMXBs

Source <sup>[a]</sup> (12)	$\nu_1$ <sup>[b]</sup> (Hz)	$\nu_2$ <sup>[c]</sup> (Hz)	$\nu_s$ <sup>[d]</sup> (Hz)	$r$ <sup>[e]</sup> (km)	$r_{\text{co}}$ <sup>[f]</sup> (km)	$Y$ <sup>[g]</sup> — ( $\equiv \frac{r}{r_{\text{co}}}$ )	$\delta r$ <sup>[h]</sup> (km) ( $\equiv r_{\text{co}} - r$ )	References
AMXP (2)								
SAX J1808.4-3658	435 ~ 567	599 ~ 737	401 (AN)	21 ~ 24	31	0.67 ~ 0.77	7 ~ 10	[1, 13]
XTE J1807.4-294	106 ~ 370	337 ~ 587	191 (A)	25 ~ 36	53	0.47 ~ 0.68	17 ~ 28	[2, 13]
Atoll (10)								
4U 0614+09	153 ~ 843	449 ~ 1162	415 (N)	16 ~ 30	31	0.50 ~ 0.95	2 ~ 16	[3, 14]
4U 1608-52	473 ~ 867	799 ~ 1104	619 (N)	16 ~ 20	24	0.68 ~ 0.84	4 ~ 8	[4, 13]
4U 1636-53	529 ~ 979	823 ~ 1228	581 (N)	15 ~ 20	25	0.61 ~ 0.79	5 ~ 10	[5, 13]
4U 1702-43	722	1055	330 (N)	17	37	0.46	20	[6, 13]
4U 1728-34	308 ~ 894	582 ~ 1183	363 (N)	16 ~ 25	34	0.45 ~ 0.73	9 ~ 19	[7, 13]
4U 1915-05	224 ~ 707	514 ~ 1055	270 (N)	17 ~ 27	42	0.40 ~ 0.65	15 ~ 25	[8, 13]
Aql X-1	795 ~ 803	1074 ~ 1083	550 (AN)	~ 17	26	0.64	~ 9	[9, 13]
IGR J17191-2821	681 ~ 870	1037 ~ 1185	294 (N)	16 ~ 17	40	0.39 ~ 0.43	23 ~ 24	[10, 13]
KS 1731-260	898 ~ 903	1159 ~ 1183	524 (N)	~ 16	27	0.58 ~ 0.59	~ 11	[11, 13]
SAX J1750.8-2900	936	1253	601 (N)	15	25	0.61	10	[12, 13]

<sup>[a]</sup> Source with both the detected twin kHz QPOs and the inferred NS spin frequency.

<sup>[b]</sup>  $\nu_1$ — Frequency of the lower kHz QPO.

<sup>[c]</sup>  $\nu_2$ — Frequency of the upper kHz QPO.

<sup>[d]</sup>  $\nu_s$ — NS spin frequency inferred from periodic or nearly periodic X-ray oscillations. A: accretion-powered millisecond pulsar. N: nuclear-powered millisecond pulsar.

<sup>[e]</sup>  $r$ — Emission radius of the twin kHz QPOs inferred by equation (2) (i.e.  $r = (\frac{GM}{4\pi^2})^{1/3} \nu_2^{-2/3}$  with  $M$  is assumed to be  $1.6 M_\odot$ ).

<sup>[f]</sup>  $r_{\text{co}}$ — Co-rotation radius inferred by equation (4) (i.e.  $r_{\text{co}} = (\frac{GM}{4\pi^2})^{1/3} \nu_s^{-2/3}$  with  $M$  is assumed to be  $1.6 M_\odot$ ).

<sup>[g]</sup>  $Y$ — Position parameter ( $Y \equiv \frac{r}{r_{\text{co}}}$ , see equation (5)).

<sup>[h]</sup>  $\delta r$ —  $\delta r \equiv r_{\text{co}} - r$ .

REFERENCES.— [1] van Straaten et al. 2005, Wijnands et al. 2003, Bult & van der Klis 2015; [2] Linares et al. 2005, Zhang et al. 2006b; [3] van Straaten et al. 2000, van Straaten et al. 2002, Bouterlier et al. 2009; [4] van Straaten et al. 2003, Barret et al. 2005, Jonker, Méndez & van der Klis 2000, Méndez et al. 1998; [5] Altamirano et al. 2008, Wijnands et al. 1997a, Bhattacharyya 2010, Di Salvo et al. 2003, Jonker, Méndez & van der Klis 2000, Jonker et al. 2002, Lin et al. 2011, Sanna et al. 2014; [6] Markwardt et al. 1999; [7] Di Salvo et al. 2001, van Straaten et al. 2002, Strohmayer et al. 1996, Migliari et al. 2003, Jonker, Méndez & van der Klis 2000, Méndez & van der Klis 1999; [8] Boirin et al. 2000; [9] Barret et al. 2008; [10] Altamirano et al. 2010; [11] Wijnands & van der Klis 1997; [12] Kaaret et al. 2002; [13] Reference in Bouterlier & Lamb 2008; [14] Strohmayer et al. 2008.

the NS spin frequency (i.e.  $\nu_K = \nu_s$ ). By setting equation (1) to be equal to  $\nu_s$ ,  $r_{\text{co}}$  can be derived as:

$$r_{\text{co}} = \left(\frac{GM}{4\pi^2}\right)^{1/3} \nu_s^{-2/3} \approx 32(\text{km}) \left(\frac{M}{1.6 M_\odot}\right)^{1/3} \left(\frac{\nu_s}{400 \text{ Hz}}\right)^{-2/3}, \quad (4)$$

where  $\nu_s$  is the NS spin frequency, and 400 Hz is the average frequency of the detected spins of NS-LMXBs (see Wang et al. 2014 for the details). We infer the co-rotation radii of the 12 sources in Table 1 by equation (4) with the NS spin frequency  $\nu_s$  and the assumed NS mass of  $1.6 M_\odot$ . The inferred  $r_{\text{co}}$  values of the 12 sources and their corresponding positions are shown in Table 1 and Fig.1, respectively. We also show the CDF curve of all the 12  $r_{\text{co}}$  values ( $r_{\text{co}} \sim 24 - 53$  km) in Fig.2 (b), from which it can be seen that 5 sources (42% of the data) share the  $r_{\text{co}}$  range of  $\sim 24 - 30$  km, 6 sources (50% of the data) share the range of  $\sim 30 - 43$  km, and the source XTE J1807.4-294 has the largest co-

rotation radius of  $\sim 53$  km. The average co-rotation radius of all listed sources is  $\langle r_{\text{co}} \rangle \sim 32$  km.

### 3.3 Position parameter

We introduce a ratio parameter  $Y$  to study the relative position relation between the emission radius of the kHz QPOs and co-rotation radius quantitatively:

$$Y \equiv \frac{r}{r_{\text{co}}} = \left(\frac{\nu_s}{\nu_2}\right)^{2/3}, \quad (5)$$

which depends on the frequencies of  $\nu_2$  and  $\nu_s$ .

For each pair of kHz QPOs in Table 1, we calculate its corresponding position parameter  $Y$  by equation (5) with  $\nu_2$  and  $\nu_s$  values. The ranges of the inferred  $Y$  values of the 12 sources are shown in Table 1, the CDF curve of which is shown in Fig.3. The range of  $Y$  is found to be  $Y \sim 0.39 - 0.95$ , or all  $Y$  values are less than unity. In other words, the

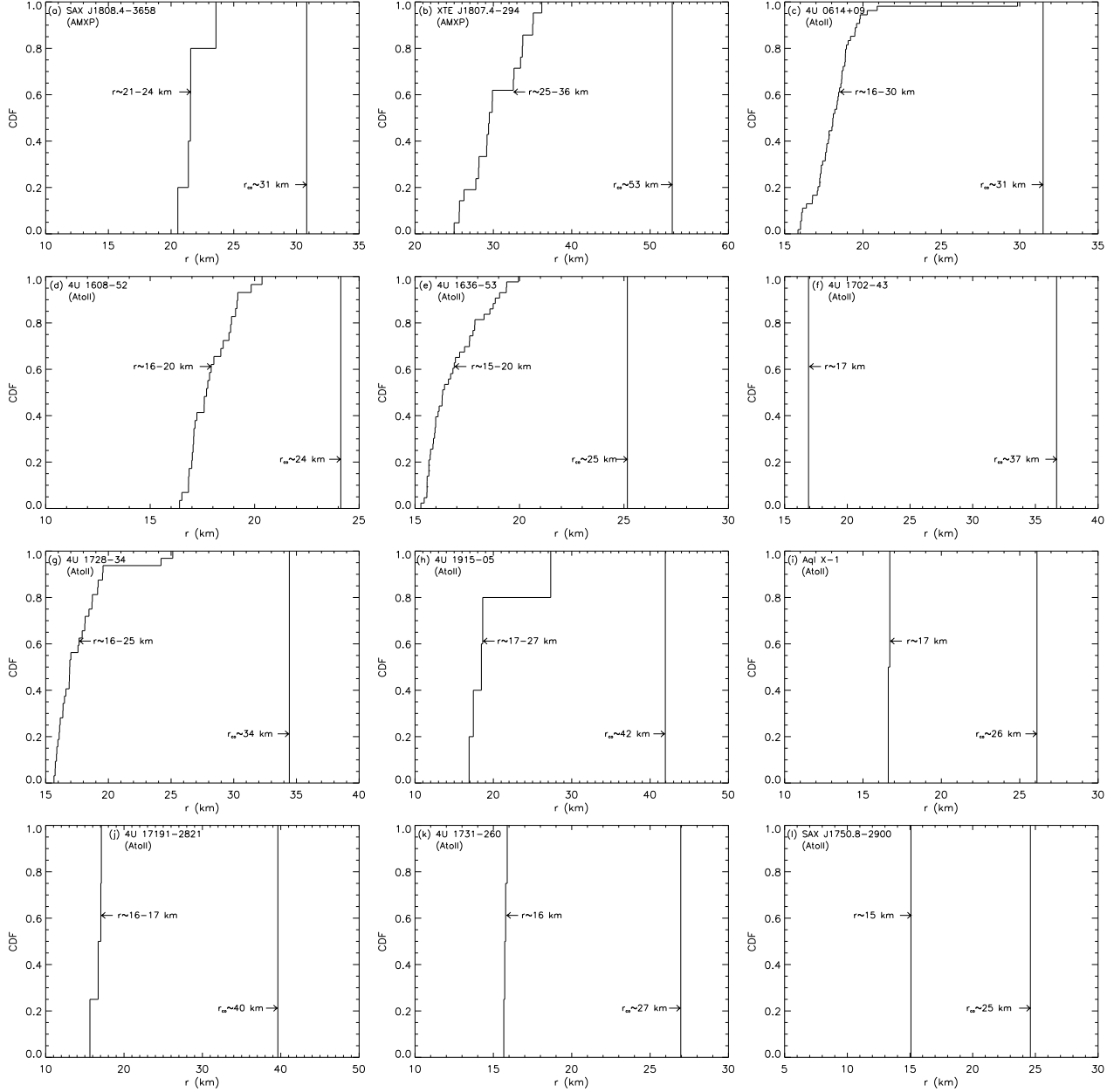


**Figure 1.** The CDF curve of the emission radius  $r$  of twin kHz QPOs, as well as the position of the co-rotation radius  $r_{co}$ , for (a) SAX J1808.4-3658 ( $r \sim 21 - 24$  km,  $r_{co} \sim 31$  km), (b) XTE J1807.4-294 ( $r \sim 25 - 36$  km,  $r_{co} \sim 53$  km), (c) 4U 0614+09 ( $r \sim 16 - 30$  km,  $r_{co} \sim 31$  km), (d) 4U 1608-52 ( $r \sim 16 - 20$  km,  $r_{co} \sim 24$  km), (e) 4U 1636-53 ( $r \sim 15 - 20$  km,  $r_{co} \sim 25$  km), (f) 4U 1702-43 ( $r \sim 17$  km,  $r_{co} \sim 37$  km), (g) 4U 1728-34 ( $r \sim 16 - 25$  km,  $r_{co} \sim 34$  km), (h) 4U 1915-05 ( $r \sim 17 - 27$  km,  $r_{co} \sim 42$  km), (i) Aql X-1 ( $r \sim 17$  km,  $r_{co} \sim 26$  km), (j) IGR J17191-2821 ( $r \sim 16 - 17$  km,  $r_{co} \sim 40$  km), (k) KS 1731-260 ( $r \sim 16$  km,  $r_{co} \sim 27$  km), (l) SAX J1750.8-2900 ( $r \sim 15$  km,  $r_{co} \sim 25$  km).

emission radii of kHz QPOs of all the sources are smaller than their co-rotation radii.

Moreover, we also investigate the innermost emission position of the kHz QPOs by analyzing the minimum of parameter  $Y$  ( $\min(Y)$ ). Fig.4 shows the CDF curve of the minima of parameter  $Y$  of 12 sources, from which we notice that the minima of  $Y$  lie in the range of  $\sim 0.39 - 0.67$  with the average value of  $\sim 0.54$ .

## 4 DISCUSSIONS AND CONCLUSIONS

Based on the data of 12 sources with the simultaneously detected twin kHz QPOs and NS spins, we investigate the relation between the emission radii of twin kHz QPOs and co-rotation radii, and find that most of the emission positions of twin kHz QPOs cluster around  $\sim 15 - 20$  km, with the average co-rotation radius of  $\langle r_{co} \rangle \sim 32$  km. The details of the conclusions and discussions are summarized as follow:

- (1) We analyze the ratios between the emission radius of

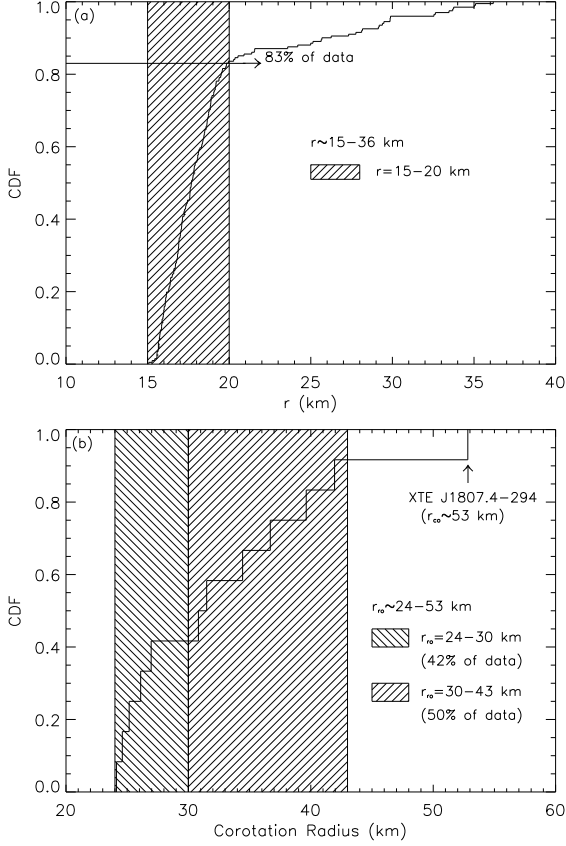


**Figure 2.** (a) The CDF curve of the emission radius  $r$  of all the twin kHz QPOs in Table 1 ( $r \sim 15 - 36$  km). The shaded area shows the radius range of  $15 - 20$  km, which contains  $\sim 83\%$  of the data. (b) The CDF curve of the co-rotation radius  $r_{co}$  of all the 12 sources in Table 1 ( $r_{co} \sim 24 - 53$  km). The shaded areas show the radius range of  $24 - 30$  km and  $30 - 43$  km respectively, which contains 42% and 50% of the data respectively. The arrow indicates the position of the co-rotation radius ( $r_{co} \sim 53$  km) of source XTE J1807.4-294.

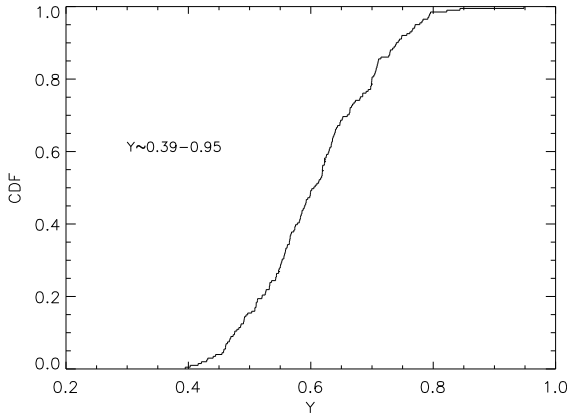


**Figure 3.** The CDF curve of all the position parameter  $Y$  in Table 1 ( $Y \sim 0.39 - 0.95$ ).

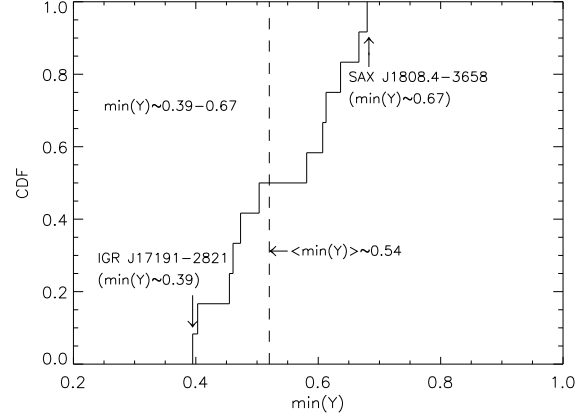


**Figure 4.** The CDF curve of the minima of the position parameter  $Y$  for all the 12 sources ( $\min(Y) \sim 0.39 - 0.67$  with the average value of  $\langle \min(Y) \rangle \sim 0.54$ ).

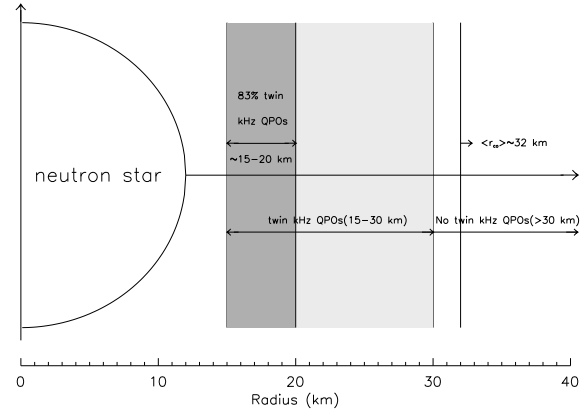


**Figure 5.** The schematic diagram of the average co-rotation radius and the emission position of twin kHz QPOs. The average co-rotation radius of the 12 sources is  $\langle r_{co} \rangle \sim 32$  km, and the emission radii of twin kHz QPOs are in the range of  $\sim 15 - 30$  km, and 83% of which are in the range of  $\sim 15 - 20$  km.

the kHz QPOs and co-rotation radius ( $Y \equiv \frac{r}{r_{co}} < 1$ , see Table 1 and Fig.3 for the details), and find that all the twin kHz QPOs are produced inside the co-rotation radii. This result indicates that the emission of twin kHz QPOs may be related to the spin-up process of accreting NS. Furthermore,  $\sim 83\%$  of the inferred emission radii of twin kHz QPOs cluster around the NS surface at  $r \sim 15 - 20$  km (see also Fig.2 (a)), which indicates that the twin kHz QPOs produce when the accreting matter collides with the hard surface or environment with the local strong magnetic field (Zhang & Kojima 2006). In particular, 4U 1608-52 shows the emission radii of twin kHz QPOs to be  $r \sim 16 - 20$  km (see Fig.1d) while the corresponding lower kHz QPO frequencies are in range of 473-867 Hz (as listed in Table 1). For this wide range of lower kHz QPO frequencies, the X-ray spectrum changes significantly. For instance, Barret (2013) has shown that the comptonization parameters are related to the lower kHz QPOs for the source 4U 1608-52, and he also estimated the inner accretion disk radius in the range of  $\sim 15 - 25$  km. Hence our proposed ac-

cretion disk structure is consistent with the result from the observed X-ray spectrum. It is noticed that parts of the sources in the sample are also observed the single kHz QPOs (e.g. van Straaten et al. 2000), which show the larger frequency range (some ones lie in the frequency range of the upper kHz QPOs) compared with the twin kHz QPOs (van der Klis 2000). The larger frequency range indicates that the single kHz QPOs may have the larger range of the emission positions, i.e. inside or outside the co-rotation radius, hence implying that the occurrence condition of single kHz QPOs is not as rigorous as the twin ones.

- (2) The Keplerian frequency  $\nu$  and the radius  $r$  of the matter in the accretion disk has the following relation (Zhang 2004; van der Klis 2006):

$$\nu \sim r^{-3/2}, \quad (6)$$

which can be written into a variation form in the following:

$$\frac{\delta\nu}{\nu} \sim \frac{3}{2} \frac{\delta r}{r}, \quad (7)$$

where  $\delta r$  and  $\delta\nu$  are set as  $\delta r = r_{\text{co}} - r$ ,  $\delta\nu = \nu - \nu_s$ . The inferred minimum ranges of  $\delta r$  for all the 12 sources are shown in Table 1,  $\min(\delta r) \sim 2$  km. Substituting  $\langle r_{\text{co}} \rangle \sim 32$  km and  $\min(\delta r) \sim 2$  km into equation (7), one can obtain  $\frac{\delta\nu}{\nu} \sim \frac{3}{2} \frac{\min(\delta r)}{\langle r_{\text{co}} \rangle} \sim 10\%$ , which indicates that the twin kHz QPOs will not occur until the upper kHz QPO frequency is bigger than NS spin frequency by 10%. We guess that the emission of twin kHz QPOs may be related to the sufficient velocity difference between the Keplerian motion of the accretion matter and NS spin. Fig.5 shows the schematic diagram of the emission position of twin kHz QPOs: As the accretion matter goes through the co-rotation radius, the twin kHz QPOs will not emit until the distance difference satisfies  $\delta r \geq 2$  km. Therefore, the twin kHz QPOs occur in-between the particular boundaries, NS surface and co-rotation radius, with the boundary layer of about several kilometers, which may represents the thickness of the transitional layer of accretion disk.

- (3) As known, the less luminous source SAX J1808.4-3658 shows the smaller frequency difference of twin kHz QPOs ( $\sim 1.5$  times smaller than other sources, see e.g. Wijnands et al. 2003), and the larger emission radii of its twin kHz QPOs are found ( $r \sim 21 - 24$  km). One explanation is that this source may have the low accretion rate due to the low luminosity, which causes the accretion disk far away from the NS surface, and the twin kHz QPOs emit at the farther positions. In addition, SAX J1808.4-3658 has been measured with the light NS mass ( $< 1.4 M_{\odot}$ , see Elebert et al. 2009), which is smaller than the average value of the millisecond pulsars of 1.6 solar mass (Zhang et al. 2011), making its Keplerian frequency systematically lower than those of other sources.

## ACKNOWLEDGMENTS

This work is supported by the National Basic Research Program of China (2012CB821800), the National Natural

Science Foundation of China NSFC(11173034, 11173024, 11303047, 11565010), the Science and Technology Foundation of Guizhou Province (Grant No.J[2015]2113 and No.LH[2016]7226), the Doctoral Starting up Foundation of Guizhou Normal University 2014 and the Innovation Team Foundation of the Education Department of Guizhou Province under Grant Nos. [2014]35.

## REFERENCES

- Abramowicz M. A. et al., 2003a, *A&A*, 404, L21  
 Abramowicz M. A. et al., 2003b, *PASJ*, 55, 467  
 Alpar M.A., 2012, *MNRAS*, 423, 3768  
 Altamirano D. et al., 2008, *ApJ*, 685, 436  
 Altamirano D. et al., 2010, *MNRAS*, 401, 223  
 Barret D. et al., 2005, *MNRAS*, 357, 1288  
 Barret D., Boutelier M., Miller M. C., 2008, *MNRAS*, 384, 1519  
 Barret D., 2013, *ApJ*, 770, 9  
 Belloni T., Psaltis D., van der Klis M., 2002, *ApJ*, 572, 392  
 Belloni T., Méndez M., Homan J., 2005, *A&A*, 437, 209  
 Belloni T., Méndez M., Homan J., 2007, *MNRAS*, 376, 1133  
 Bhattacharya D., van den Heuvel E.P.J., 1991, *Physics Reports*, 203, 1  
 Bhattacharyya S., 2010, *Research in Astronomy and Astrophysics*, 10, 227  
 Boirin L. et al., 2000, *A&A*, 361, 121  
 Boutelier M., Barret D., Miller M. C., 2009, *MNRAS*, 399, 1901  
 Boutiloukos S., Lamb F. K., 2008, in Bassa C. G. et al., eds, 40 Years of Pulsars: Millisecond Pulsars, Magnetars, and More, AIP Conf. Ser. Vol. 983. Am. Inst. Phys., Melville, NY, p. 533  
 Bult P. & van der Klis M., 2015, *ApJ*, 798, L29  
 Burderi L. et al., 2006, *ApJ*, 653, L133  
 Burderi L. & Di Salvo T., 2013, *Memorie della Societa Astronomica Italiana*, 84, 117  
 Di Salvo T. et al., 2001, *ApJ*, 546, 1107  
 Di Salvo T., Méndez M., van der Klis M., 2003, *A&A*, 406, 177  
 Elebert P. et al., 2009, *MNRAS*, 395, 884  
 Ford E. C., van der Klis M., Kaaret P., 1998a, *ApJ*, 498, L41  
 Ford E. C. et al., 1998b, *ApJ*, 508, L155  
 Ford E. C., van der Klis M., 1998, *ApJ*, 506, L39  
 Ford E. C. et al., 2000, *ApJ*, 537, 368  
 Ghosh P., Lamb F. K., 1979, *ApJ*, 234, 296  
 Hasinger G., van der Klis M. 1989, *A&A*, 225, 79  
 Homan J. et al., 2002, *ApJ*, 568, 878  
 Jonker P. G., Méndez M., van der Klis M., 2000, *ApJ*, 540, L29  
 Jonker P. G. et al., 2000, *ApJ*, 537, 374  
 Jonker P. G., Méndez M., van der Klis M., 2002, *MNRAS*, 336, L1  
 Kaaret P. et al., 1998, *ApJ*, 497, L93  
 Kaaret P. et al., 2002, *ApJ*, 575, 1018  
 Kluźniak W., Michelson P., Wagoner R. V., 1990, *ApJ*, 358, 538  
 Kluźniak W., Abramowicz M. A., 2001, *Acta Phys. Polonica B*, 32, 3605  
 Lamb F. K., Miller M. C., 2001, *ApJ*, 554, 1210

Lin Y. F. et al., 2011, ApJ, 726, 74  
 Linares M. et al., 2005, ApJ, 634, 1250  
 Liu Q. Z. et al., 2007, A&A, 469, 807  
 Markwardt C. B., Strohmayer T. E., Swank, J. H., 1999, ApJ, 512, L125  
 Mauche C. W., 2002, ApJ, 580, 423  
 Méndez M. et al., 1998, ApJ, 505, L23  
 Méndez M., van der Klis M., 1999, ApJ, 517, L51  
 Méndez M. et al., 1999, ApJ, 511, L49  
 Méndez M., van der Klis M., E. C. Ford, 2001, MNRAS, 321, 1016  
 Migliari S., van der Klis M., Fender R. P., 2003, MNRAS, 345, L35  
 Miller M. C., Lamb F. K., Psaltis D., 1998, ApJ, 508, 791  
 Miller M. C., 2002, Nat, 420, 31  
 Miller M. C., & Miller J.M., 2015, PhR, 548, 1  
 Osherovich V., & Titarchuk L., 1999, ApJ, 522, L113  
 Peille P., Olive J.F., & Barret D., 2014, A&A, 567, 80  
 Psaltis D., Belloni T., & van der Klis M. 1999, ApJ, 520, 262  
 Sanna A. et al., 2014, MNRAS, 440, 3275  
 Shapiro S. L., Teukolsky S. A., 1983, Black Holes, White Dwarfs, and Neutron Stars: The Physics of Compact Objects. Wiley Interscience, New York  
 Smale A. P., Zhang W., White N. E., 1997, ApJ, 483, L119  
 Stella L., Vietri M., 1999, Phys. Rev. Lett., 82, 17  
 Stella L., Vietri M., Morsink S. M., 1999, ApJ, 524, L63  
 Strohmayer T. E. et al., 1996, ApJ, 469, L9  
 Strohmayer T. E., Markwardt C. B., Kuulkers E., 2008, ApJ, 672, L37  
 Stuchlík Z. et al., 2015, Acta Astronomica, 65, 169  
 Török G. et al., 2005, A&A, 436, 1  
 van der Klis M. et al. 1996, ApJ, 469, L1  
 van der Klis M., 2000, ARA&A, 38, 717  
 van der Klis M., 2006, in Lewin W. H. G., van der Klis M., eds, Compact Stellar X-Ray Sources, Cambridge Univ. Press, Cambridge, p.39  
 van der Klis M., 2016, invited talk in European Week of Astronomy and Space Science 2016, Timing Low-Mass X-Ray Binaries and Accreting Millisecond Pulsars, 4-8 July 2016, Athens Greece  
 van Straaten S. et al., 2000, ApJ, 540, 1049  
 van Straaten S. et al., 2002, ApJ, 568, 912  
 van Straaten S., van der Klis M., Méndez M., 2003, ApJ, 596, 1155  
 van Straaten S., van der Klis M., Wijnands R., 2005, ApJ, 619, 455  
 Walter R. et al., 2015, A&ARv, 23, 2  
 Wang D.H. et al., 2013, MNRAS, 435, 3494  
 Wang D.H. et al., 2014, Astron. Nachr., 335, 168  
 Wang D.H. et al., 2015, MNRAS, 454, 1231  
 Warner B., & Woudt P. A., 2002, in ASP Conf. Ser. 261, The Physics of Cataclysmic Variables and Related Objects, ed. B. T. Gänsicke, K. Beuermann, & K. Reinsch (San Francisco: ASP), 406  
 Wang J. et al., 2012, Astron. Nachr., 333, 274  
 Wijnands R. et al., 1997a, ApJ, 479, L141  
 Wijnands R. et al., 1997b, ApJ, 490, L157  
 Wijnands R., van der Klis M., 1997, ApJ, 482, L65  
 Wijnands R. et al., 1998, ApJ, 495, L39  
 Wijnands R. et al., 2003, Nat, 424, 44  
 Zhang C. M., 2004, A&A, 423, 401

Zhang C. M. et al., 2006a, MNRAS, 366, 1373  
 Zhang C.M., Kojima Y., 2006, MNRAS, 366, 137  
 Zhang C. M. et al., 2011, A&A, 527, 83  
 Zhang C. M., Wang D. H., 2013, in Zhang C. M., Belloni T., Méndez M. et al., eds, Feeding Compact Objects: Accretion on All Scales, Proceedings of the International Astronomical Union, IAU Symp. 290, Cambridge: Cambridge University Press, pp. 381-385  
 Zhang F. et al., 2006b, ApJ, 646, 1116

This paper has been typeset from a  $\text{\LaTeX}$  file prepared by the author.